Plasmonics (2012) 7:435–439
DOI 10.1007/s11468-011-9325-1

# Flat-Top Transmission Band in Periodic Plasmonic Ring Resonators

**Jin-Xiong Tan · Yang-Bo Xie · Jian-Wen Dong · He-Zhou Wang**

Received: 22 September 2011 / Accepted: 19 December 2011 / Published online: 10 January 2012


**Abstract** Flat-top transmission bands are found in a plasmonic structure constructed by periodic ring resonators. Fabry–Perot effects can be suppressed in a set of parameters determined by an effective medium method. Two kinds of transmission bands with flat-top profiles can emerge due to either ring resonance or Bragg scattering. These bands are both red shifted when the distance of rings increases. Both transfer matrix method and finite difference time domain method are utilized to investigate the flat-top bands. The proposed structure can be employed as a plasmonic band-pass filter and might be useful in the field of integrated optoelectronics.

**Keywords** Surface plasmon polariton · Optical resonator · Flat-top band

## Introduction

Surface plasmon polaritons (SPPs) are surface electromagnetic (EM) waves propagating along the interface of metal and dielectric, and their amplitudes decay exponentially from the interface [1]. SPPs have drawn considerable attention in recent years, for the reason that they serve as the promising approach to overcome diffraction limits, and they can manipulate light at sub-wavelength scale [2]. This offers important flexibility in design and fabrication of SPP-based integrated circuits for optical communications. Various kinds of plasmonic devices based on metal–insulator–metal (MIM) waveguide have been proposed [3–8]. The plasmonic filter is one of the important devices in the field of optical integrations. In the transmission band of the MIM waveguide, there are many plasmonic modes experiencing multiple interferences. So the transmission spectrum always has oscillations due to Fabry–Perot (FP) effects. As a result, a pure MIM waveguide cannot be a band-pass filter, which has a negative impact on plasmonic integrated circuits. The aim of this paper is to overcome such disadvantage in the field of integrations.

In this paper, periodic ring resonators connected by the MIM waveguide are found to possess flat-top transmission bands. There are two kinds of flat-top bands which are due to either ring resonances or Bragg scatterings, respectively. The flat-top transmission bands will occur when the distance between two neighboring rings is set to appropriate values. Both the transfer matrix method (TMM) and finite difference time domain (FDTD) method are utilized to demonstrate such behavior.

## Effective Medium Retrieval for Plasmonic Structure

Consider a plasmonic structure constructed by metallic strips and rings, as illustrated in Fig. 1. The length of the strips is $d$. The outer and inner radii of the ring are $r_a$ and $r_b$, respectively. An air waveguide with the width of $w$ is used to connect the rings. The structural size in the $y$ direction is assumed to be infinite. The EM wave with magnetic field along the $y$ direction propagates along the positive $z$ direction.

The studied structure can also be viewed as one-dimensional multilayers constructed by two kinds of metamaterials with different effective EM parameters. From this point of view, we mark the strip and the ring as effective

J.-X. Tan · Y.-B. Xie · J.-W. Dong (✉) · H.-Z. Wang
State Key Laboratory of Optoelectronic Materials and Technologies, Sun Yat-Sen (Zhongshan) University, Guangzhou 510275, China
e-mail: dongjwen@mail.sysu.edu.cn

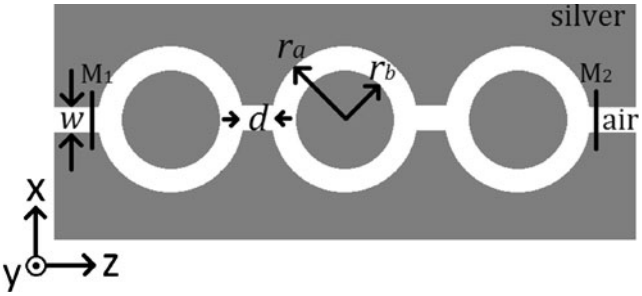


**Fig. 1** Illustration of the periodic plasmonic band-pass filter. *Gray* and *white* represent silver and air, respectively. $r_a$ and $r_b$ are the outer and inner radii of the ring. $w = r_a - r_b$ is the width of the air core. $d$ is the length of the strips. $M_1$ and $M_2$ are two monitors to detect incident power and transmitted power in FDTD simulation

medium A and B, respectively. The effective parameters of the strip can be retrieved by the dispersion of purely metallic waveguide with the following form:

$$\frac{\sqrt{\beta^2 - \varepsilon_m k_0^2}}{\varepsilon_m} = -\frac{\sqrt{\beta^2 - \varepsilon_d k_0^2}}{\varepsilon_d} \tan h(\frac{w}{2}\sqrt{\beta^2 - \varepsilon_d k_0^2})$$

where $\beta$ is the longitudinal wave number. $k_0=\omega/c$ and $\omega$ is the working frequency. $\varepsilon_d=1$ for the air core. $\varepsilon_m$ is the permittivity of the metal, characterized by the Drude model [6], $\varepsilon_m = \varepsilon_0 - \omega_p^2/\omega(\omega + i\gamma)$, where $\varepsilon_0$ is the dielectric constant at infinite angular frequency, $\omega_p$ is the bulk plasma frequency, and $\gamma$ is the damping frequency. Here, we choose silver so we have $\varepsilon_0=3.7$, $\omega_p=2{,}176$ THz, and $\gamma=4.35$ THz [6, 7]. The effective permittivity of the strip is retrieved by $\varepsilon_{eff,A} = (\beta/k_0)^2$, and the effective permeability of the strip equals to one. Figure 2a shows $\varepsilon_{eff,A}$ as a function of the working frequency at $w=100$ nm. It is found that the real part of $\varepsilon_{eff,A}$ is a weakly increasing function of the frequency, and the imaginary part is close to zero. More calculations show that both real and imaginary parts of $\varepsilon_{eff,A}$ decrease as $w$ increases.

We turn to retrieve the effective parameters of the ring. The ring can be viewed as a medium whose effective optical length is $n_{eff,B} \cdot d_{eff,B}$, where $n_{eff,B}$ is the effective refractive index, and $d_{eff,B} = \pi r_m$ is the effective thickness of the ring [9]. Here $r_m$ is the mean radius. The effective permittivity and permeability are determined by the standard procedure [10]. The effective refractive index and the effective impedance are first retrieved from the reflection and transmission coefficients calculated by the finite element method. Then the effective permittivity and permeability are obtained by their ratio and multiplication. The representative frequency relationships of the effective permittivity and the permeability are calculated for the ring with the radii of $r_a=300$ nm and $r_b=200$ nm. We find that the effective permittivity exhibits anti-resonant behavior in the frequency region from 151 to 158 THz. This is shown in Fig. 2b where the real part

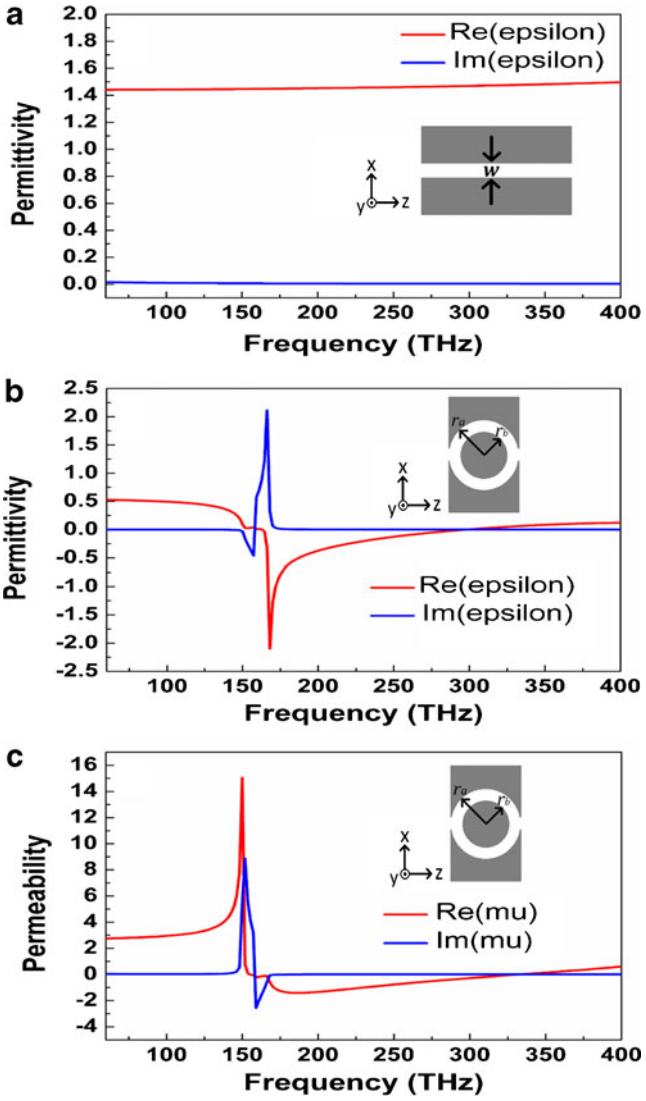


**Fig. 2** (Color online) **a** Effective permittivity of an infinite-long plasmonic strip with $w=100$ nm. **b** Effective permittivity and **c** effective permeability of the plasmonic ring with $r_a=300$ nm and $r_b=200$ nm

of effective permittivity (red) is close to zero, while the imaginary part (blue) is negative in this frequency interval. The anti-resonant region for the effective permeability is from 158 to 165 THz (Fig. 2c). The occurrence of the anti-resonant behavior is caused by finite spatial periodicity of the ring, and it is an unavoidable problem in the effective medium since the spatial periodicity is inevitable in the metamaterials [11]. We note that the retrieval procedure is a simple and efficient method to study the EM transport in the MIM system, although the procedure might have deviations near the resonant frequency region due to the comparability of the working wavelength (around 900 and 2,000 nm in this paper) and the ring size. We also note that our method can anticipate novel plasmonic devices using TMM instead of the complicated full-wave simulation.

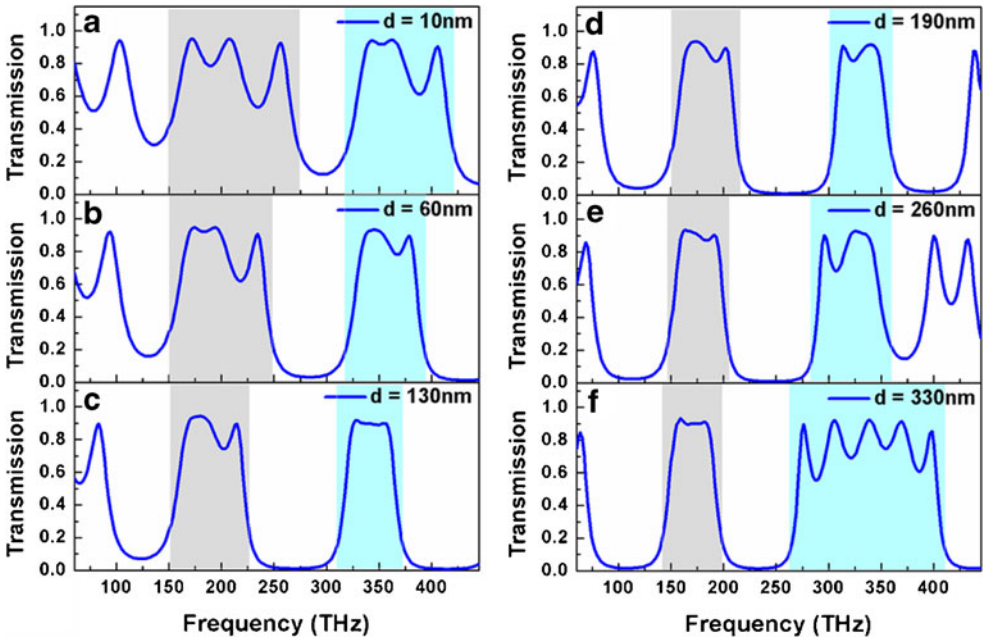


**Fig. 3** (Color online) Transmission spectra of the plasmonic filter when $d$ equals to **a** 10 nm, **b** 60 nm, **c** 130 nm, **d** 190 nm, **e** 260 nm, and **f** 330 nm. The *light gray* and *light blue* areas indicate the RP and non-RP band, respectively. The radii of the plasmonic ring are $r_a$=300 nm and $r_b$=200 *nm*. Note that flat-top transmission bands appear in **c** and **f**

## Numerical Simulations and Discussions

With the help of the effective parameters of the strip and the ring, we now study the flat-top transmission properties in the plasmonic filter shown in Fig. 1. TMM is used to calculate the transmission spectra [12]. Transmission spectra in normal incidence with different values of $d$ are shown in Fig. 3. There are two passing bands from 100 to 450 THz. One is near the anti-resonant frequency region (light gray in Fig. 3), so it is called resonant passing (RP) band. The other is out of the anti-resonant frequency region (light blue in Fig. 3), and it is a non-RP band.

When $d$ is small, the FP effects in both bands are clearly visible; see Fig. 3a. As $d$ increases, it is interesting to find that the frequency peaks in both bands can either merge together or split up. For example, as $d$ increases from 10 to 330 nm, three peaks in the RP band get closer and closer and finally merge together when $d$=330 nm. As a result, a flat-top band emerges from 156 to 184 THz, and its transmittance is as high as 90%. We expect that such a MIM ring resonator structure is a good candidate for band-pass plasmonic filters. On the other hand, the FP peaks in the non-RP band experience a more complicated process. A flat-top transmission band occurs from 325 to 357 THz when $d$= 130 nm. But when $d$ increases over 130 nm, the flat-top band is destroyed and splits into multiple peaks again. The reason is that a Bragg gap, which is well defined from 350 to 450 THz at $d$=190 nm, gradually disappears as $d$ increases from 190 to 330 nm.

In order to demonstrate the flat-top transmission behavior, we employ an FDTD simulator [13] to do two-dimensional full-wave simulations. A Gaussian source is placed at the left

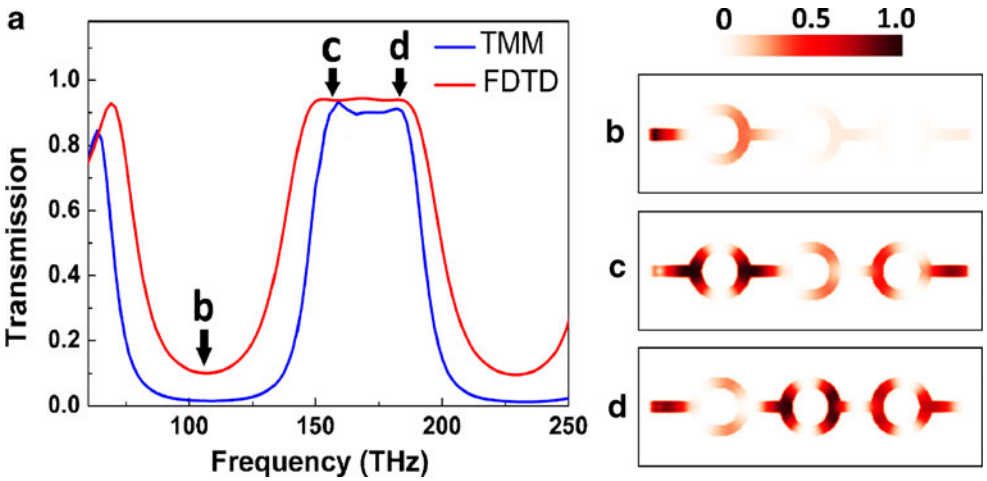


**Fig.4** (Color online) **a** Transmission spectra from the TMM (*blue*) and FDTD (*red*) method when the length of the strips is 330 nm. **b**, **c**, and **d** $|H_y|^2$ field distributions in the plasmonic filter at the frequency of 105THz, 155THz and 185THz, respectively

side of the band-pass filter. The boundaries surrounding the filter are set to be perfectly matched layers. The transmittance is defined as $T = P_{out}/P_{in}$, where $P_{in}$ and $P_{out}$ denote the incident power and transmitted power, respectively.

Figure 4 shows the FDTD results for the RP band in Fig. 3f. The flat-top transmission band calculated by the FDTD method (red) is present and is almost consistent with the TMM results (blue), although the FDTD bandwidth is a little larger than that of TMM. Figure 4c and d depicts the distributed patterns of the magnetic fields ($|H_y|^2$) at the low and high edge of the flat-top band. The EM wave can propagate through the whole filter with high transmittance. For comparison, Fig. 4b illustrates the field pattern out of the flat-top band. It is clearly seen that the fields at the exit almost vanish, so that low transmittance is recorded in the spectrum. Figure 5 shows the FDTD results for the non-RP band in Fig. 3c. The flat-top transmission band is also demonstrated. Similar pictures as those in Fig. 4 can be found. The difference is that the modes in Fig. 5 are higher order, while the modes in Fig. 4 are lower order.

We also investigate the shift of the flat-top transmission band with the increase of the strip length. Here, the edge of the transmission band is defined by 3-dB transmittance. In order to better illustrate the profile of the transmission band, we introduce the ripple factor $R = (I_{max} - I_{min})/(I_{max} + I_{min})$, where $I_{max}$ is the maximum intensity of the peak, and $I_{min}$ is the minimum intensity of the dip [14]. We fix the threshold of the ripple factor as 0.01 because the ripples within the passing band are small enough when the factor is less than 1%. Figure 6 shows the relationship between the band edge of the flat-top RP band and the strip length $d$. We find that the RP band possesses a flat-top profile when $d$ is from 250 to 400 nm, and both edges of the RP band exhibit red shift as $d$ increases. The bandwidth of the flat-top RP band is nearly unchanged. Similar characteristics are found in the non-RP band. The non-RP flat-top band is present when $d$ varies from 80 to 170 nm, if the threshold of the ripple factor is fixed to 0.03.

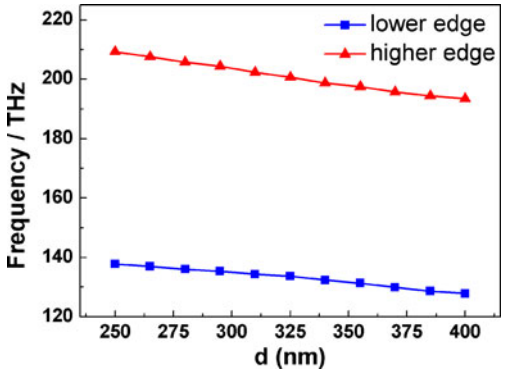


**Fig. 6** (Color online) Relationship between band edges of the RP band and the strip length $d$

## Summary

In summary, we have demonstrated that the plasmonic structure with ring resonators possesses flat-top transmission bands. The effective medium method is employed to determine each unit cell of the plasmonic structure, so that the simple TMM calculation, instead of the complicated full-wave simulation, is available in the design procedure. Two flat-top bands with high transmittance are found in the MIM ring resonators with appropriate parameters. Results of FDTD simulations are very consistent with the TMM prediction. These findings manifest the design can be utilized as a SPP-based band-pass filter, and has potential applications in nanoscale photonic and integrated optoelectrical devices.

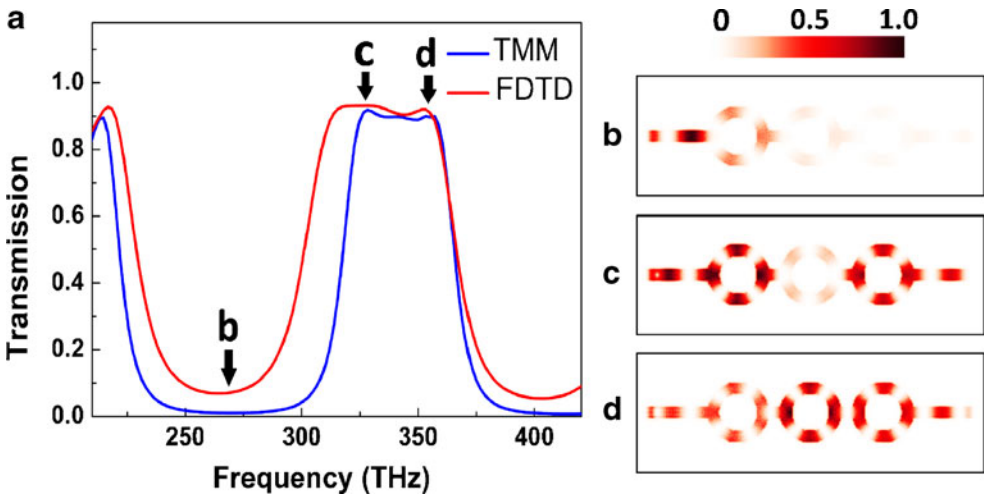


**Fig. 5** (Color online) **a** Transmission spectra from the TMM (*blue*) and FDTD (*red*) method when the length of the strips is 130 nm. **b**, **c**, and **d** $|H_y|^2$ field distributions in the plasmonic filter at the frequency of 270, 325, and 360 THz, respectively

**Acknowledgments** This work is supported by the National Natural Science Foundation of China (10804131, 11074311, 10874250), the Fundamental Research Funds for the Central Universities (2009300003161450), and the Guangdong Natural Science Foundation (10451027501005073).

## References

1. Zayats AV, Smolyaninov II, Maradudin AA (2005) Nano-optics of surface plasmon polaritons. Phys Rep 408(3–4):131–314
2. Barnes WL, Dereux A, Ebbesen TW (2003) Surface plasmon subwavelength optics. Nature 424(6950):824–830
3. Veronis G, Fan S (2005) Bends and splitters in metal-dielectric-metal subwavelength plasmonic waveguides. Appl Phys Lett 87 (13):131102
4. Lee PH, Lan YC (2010) Plasmonic waveguide filters based on tunneling and cavity effects. Plasmonics 5:417–422
5. Wang B, Wang GP (2005) Plasmon Bragg reflectors and nano-cavities on flat metallic surfaces. Appl Phys Lett 87:013107
6. Park J, Kim Hand Lee B (2008) High order plasmonic Bragg reflection in the metal-insulator-metal waveguide Bragg grating. Opt Express 16:413–425
7. Han Z, Forsberg E, He S (2007) Surface plasmon Bragg gratings formed in metal-insulator-metal waveguides. IEEE Photon Tech Lett 19:91–93
8. Liu Y, Liu Y, Kim J (2010) Characteristics of plasmonic Bragg reflectors with insulator width modulated in sawtooth profiles. Opt Express 18:11589–11598
9. Wen M, Wei ZY, Li HQ (2005) One-dimensional photonic bandgap structures by periodically loaded rings on microstrip line. Microwave Conference Proceedings, 2005. APMC 2005. Asia-Pacific Conference Proceedings, vol. 3, pp. 3, 4–7.
10. Smith DR, Vier DC, Koschny Th, Soukoulis CM (2005) Electromagnetic parameter retrieval from inhomogeneous metamaterials. Phys Rev E 71:036617
11. Koschny T, Markos P, Smith DR, Soukoulis CM (2005) Resonant and antiresonant frequency dependence of the effective parameters of metamaterials. Phys Rev E 68:065602(R)
12. Yeh P (1988) Optical waves in layered media. Wiley, New York
13. Oskooi AF, Roundy D, Ibanescu M, Bermel P, Joannopoulos JD, Johnson SG (2010) MEEP: a flexible free-software package for electromagnetic simulations by the FDTD method. Comput Phys Commun 181:687–702
14. Levy M, Yang HC, Steel MJ, Fujita J (2001) Flat-top response in one-dimensional magnetic photonic bandgap structures with Faraday rotation enhancement. J Lightwave Technol 19:1964–1969